Natural Resources for Human Health

visagaa publishing house

Original Research

View Article online

Check for updates

Received 27 December 2025
Revised 27 January 2026
Accepted 29 January 2026
Available Online 13 July 2026

Edited by Ricardo Diego de Albuquerque

KEYWORDS:
Quality control
Phenolic acids
Phytochemical profiling
St. John's wort
Anatomical analysis
Secretory structures

https://doi.org/10.53365/nrfhh/217529
eISSN: 2583-1194

A Comprehensive Pharmacognostical, Phytochemical, and Mechanistic Evaluation of *Hypericum perforatum* Root Extracts for Epilepsy Using Integrated Bioinformatic Approaches

Pooja Sinoriya[1,*], Milind Sharad Pande[2], Nitin Kumar[3]

[1]Department of Pharmacy, IIMT College of Medical Sciences, IIMT University, Ganga Nagar, Meerut, Uttar Pradesh, India
[2]Department of Pharmacognosy, IIMT College of Medical Sciences, IIMT University, Ganga Nagar, Meerut, Uttar Pradesh, India
[3]IIMT College of Pharmacy, Greater Noida, Uttar Pradesh, India

ABSTRACT: *Hypericum perforatum* L. is a well-documented medicinal plant traditionally used for neurological and inflammatory disorders. However, comprehensive quality standardization and mechanistic validation of its root extracts is prohibited. The present study aimed to establish pharmacognostical and phytochemical standardization for *Hypericum perforatum* roots and to elucidate their potential antiepileptic properties using an integrated analytical and bioinformatic approach. Pharmacognostical evaluation included physicochemical parameters, such as ash values and extractive values, supported by qualitative phytochemical screening. Regarding densitometric profiling and quantitative quercetin quantification, high-performance thin-layer chromatography was employed, ensuring batch-to-batch consistency and confirmation of marker compounds. Comprehensive characterization of metabolites proved possible by liquid chromatography–mass spectrometry analysis, which validated the physical presence of important biologically active compounds, such as rutin, quercetin, kaempferol, gallic acid, and ferulic acid. To explore the molecular basis of antiepileptic activity, identified phytochemicals were subjected to network pharmacology investigation. In network pharmacology, protein–protein interaction and enhancement investigation revealed the key targets, such as prostaglandin-endoperoxide synthase 2 (*PTGS2*), *AKT1*, epidermal growth factor receptor (*EGFR*), *ESR1*, *BCL2*, and *SRC*, which were involved in neuronal excitability, oxidative stress, inflammation, and apoptotic regulation. Integrated Kyoto Encyclopedia of Genes and Genomes and gene ontology analysis highlighted estrogen signaling, *EGFR*-related pathways, oxidative stress response, and kinase-mediated signaling as major mechanisms relevant to epilepsy.

* Corresponding author.
E-mail address: psinoriya@gmail.com (Pooja Sinoriya)

INTRODUCTION

Phytomedicine, also known as "alternative medicine," refers to the use of plant metabolites in mixtures that contain pharmacologically active compounds exhibiting therapeutic properties. The plant parts used for phytomedicines include barks, leaves, roots, tubers, stems, herbs, flowers, fruits, exudates, and plant extracts. Over the last decade, significant interest has been observed in the use of medicinal plant products. Consequently, numerous plant peptides are shown to have beneficial as well as positive effects on human health. The combination of bioactive compounds present in plants is usually responsible for the medicinal effects of plant materials. These medicinal properties are often unique to specific plant species or groups (Coopoosamy et al., 2023). Research has indicated numerous advantageous features of herbal medicines. Despite being scientifically established by trial and error, several herbal treatments have been demonstrated as extremely successful. According to a recent study, 39% of the 520 medications approved between 1983 and 1984 were from natural medicine, natural content, and natural goods, and 60–80% of the antibacterial and antiviral qualities in pharmaceutical compounds were derived from natural substances (Dhanave et al., 2024).

Hypericum was first described in ancient Greece by Hippocrates (Theodorakopoulou et al., 2025). *Hypericum perforatum* L. known as St. John's wort, belonging to the family *Hypericaceae*, is a medicinal plant, historically utilized by both traditional and modern medicinal practices (Rayhaneh Amooaghaie, 2025; Shafaei, 2026). *Hypericum perforatum* is a herbaceous perennial plant species that grows extensively in both tropical and temperate climates, particularly in Europe, Asia, India, North Africa, and North America (Behroozilak et al., 2025; Kurt et al., 2025). This plant typically attains a height of approximately 50–100 cm. The common name is derived from St. John's wort, a Baptist plant, with flowers traditionally used throughout the celebration season.

Perforatum species refers to elliptical leaves which exhibit numerous translucent glands that impart a perforated appearance against light. Medicinally important parts include leaves and flowers, and still sealed flower buds are usually harvested in late spring or in early summer season. These plant material must be dried promptly under warm conditions to prevent degradation of bioactive components (Drożdżał et al., 2025). Several pharmacological properties of *Hypericum perforatum* and other *Hypericum* species as reported in previous studies include anti-ageing, antioxidant, antineoplastic, antidepressant, anti-inflammatory, antimicrobial, analgesic, wound-healing, and cytotoxic (Górnaś and Siger, 2025; Górnaś et al., 2025; Maslov et al., 2025).

Chemical composition of *Hypericum perforatum* extract has been investigated extensively, leading to the identification of numerous secondary metabolites, such as rutin, hyperforin, hyperoside, quercitrin, isoquercitrin, quercetin, hypericin, and chlorogenic acid (Alahmad et al., 2022; Al Nooh et al., 2025). Among these, hyperforin and hypericin have been valuable components for the pharmaceutical industry (Gokcek-Sarac and Altunkaya, 2025; Rizzo et al., 2020). Hypericin, being a major bioactive compound of *Hypericum perforatum*, has shown significant prospective photodynamic properties of a photosensitive agent (Amooaghaie and Rajaie, 2025). However, inadequate solubility, significant lipophilicity, pH variability, and prohibitive manufacturing expenses have restricted its beneficial effectiveness (Ma et al., 2025). On the other hand, hyperforin is a significant immune-modulating antimicrobial agent. It demonstrates a broad spectrum of antibacterial properties against antibiotic-resistant Gram-positive and some Gram-negative infections, elevates phagocytic activity, and stimulates the breakdown of bacteria of human multifaceted neutrophils. (Schmidt-Przewoźna et al., 2025). Notably, hyperforin is capable of crossing critical physiological barriers, including the blood–brain barrier, which underscores its therapeutic potential in the management of infections, such as meningitis and gonorrhoea, particularly in immunocompromised patients, including those of acquired immunodeficiency syndrome (AIDS) (Kilibarda et al., 2025).

The phytochemical profile of *Hypericum perforatum* is attributed to the presence of multiple classes of bioactive compounds, such as naphthodianthrones, phloroglucinol derivatives, flavonoids, and xanthones (Jin et al., 2025). Researchers are especially engaged in discovering drugs for the overall human health because of a wide range of chemical properties and an array identified among these plants. Research interest and clinical relevance of *Hypericum perforatum* in neurodegenerative disorders have increased markedly in recent years. Alzheimer's disease, Parkinson's syndrome, and Huntington's disease (HD) have been more prevalent in the elderly population. These conditions are characterized by a progressive degeneration of neurons in the nervous system, resulting in a gradual impairment of cognitive and physical abilities. Owing to the complex etiology of neurodegenerative diseases and the limited efficacy of currently available therapies, there is an urgent need to explore novel treatment strategies to reduce their growing medical and social burden. Consequently, investigations of new therapeutic modalities derived from medicinal plants, such as *Hypericum perforatum*, represent a promising approach for addressing this unmet clinical need (Suryawanshi et al., 2024). Most studies suggest that the pharmacological effects of *Hypericum perforatum* are primarily associated with the inhibition of serotonin reuptake at neuronal synapses and

suppression of monoamine oxidase activity. At present, a wide range of phyto and nutraceutical formulations, including tinctures, teas, and juices containing St. John's wort, are available commercially (Borawska et al., 2016).

2. MATERIAL AND METHODS

2.1. Collection of plant material

Hypericum perforatum roots were collected in Haldwani, Uttarakhand, India, in November 2023. The plant was identified and authenticated as *Hypericum perforatum* (Family *Hypericaceae*) by Prof. Vijai Malik, Head of the Department of Botany at Chaudhary Charan Singh University, Meerut, Uttar Pradesh, India, where a voucher specimen Bot/PB/536 was deposited.

2.2. Chemicals

All reference chemicals and solvents used for high-performance thin-layer chromatography (HPTLC) and liquid chromatography–mass spectrometry (LC-MS) analysis were procured from Arbro Pharmaceuticals Ltd., New Delhi, India, and the Indian Institute of Technology, Roper, Punjab, India. Other chemicals, such as chloroform, methanol, benzene, ethanol, and acetone, were purchased from Azytus Material Sciences Pvt. Ltd., Secunderabad, Telangana, IBuyChemikals, Chennai, and LABWale, New Delhi, India. The investigation utilized purely analytical-grade chemicals and solvents.

2.3. Preparation of extract

Roots of *Hypericum perforatum* were thoroughly washed, shade-dried, and powdered coarsely. A total of 100 g of the powdered material was used. Successive extraction was carried out utilizing Soxhlet apparatus extracted with their polarity solvents in increasing order such as benzene, chloroform, acetone, ethanol, or methanol (Abubakar, 2020). For extraction, a drug–solvent ratio of 1:4 (w/v) was maintained (100 g plant powder with 400 mL solvent) (Monagas et al., 2022). After extraction, the respective solvent was recovered and concentrated under reduced pressure. The residue (marc) was air-dried before proceeding to the next solvent. All concentrated extracts were stored in labeled amber bottles at 4°C for further phytochemical screening. Based on a literature review and the identification of prominent compounds in each extract, both acetone and ethanol extracts were selected for further detailed investigations (Palaiogiannis et al., 2023).

2.4. Pharmacognostic evaluation

2.4.1. Morphological study

The roots of *Hypericum perforatum* L., washed thoroughly and shade-dried at room temperature, were examined for macromorphological parameters, such as color, shape, size, texture, and organoleptic properties, such as taste and odor, by following standard pharmacognostical guidelines (Adom et al., 2022).

2.4.2. Microscopical study

Thin slices of *Hypericum perforatum* roots were cut manually, washed with distilled water, and placed on a slide with a few drops of safranin and glycerin. A coverslip was placed on the slide, and the sample was viewed under a microscope at 10× magnification and photographed (Klangprapun et al., 2018; Swingle et al., 2024).

A small amount of fine powder of *Hypericum perforatum* root was placed on a slide with one drop of glycerine and covered with a coverslip. The sample was examined under microscope and photographed (Limpabandhu et al., 2024b).

2.5. Physiochemical parameters

To determine moisture content or loss on drying, acid-insoluble ash, water-soluble total ash, and alcohol-soluble extractive value of *Hypericum perforatum*, dried powdered sample were used. To determine moisture content, about 5 g of sample was analyzed using a moisture balance (Limpabandhu et al., 2024a). For total ash, 2 g of sample was incinerated in a silica crucible at 650°C until it turned white, representing absence of carbon. The total amount of ash was measured. For acid-insoluble ash, 25 mL of diluted HCL was used to boil entire amount of ash. Insoluble material was collected on ashless filter paper, cleaned with hot water, dried, and weighed (Fan et al., 2024).

Furthermore, for determining water-soluble and alcohol-soluble extractive of the plant, 5 g of the sample was dissolved separately in 100 mL of water and alcohol, and the contents were sonicated for 3 h, filtered, and concentrated (25 mL out of 100 mL) in a water bath at 105°C till dried extracts were obtained. The obtained extracts were weighed and calculated (Gempo et al., 2024):

$$\text{Total ash} = \frac{\text{Weight of petri dish with extract} - \text{Weight of empty dish}}{\text{Weight of the drug}} \times 100.$$

$$\text{Acid-insoluble ash} = \frac{\text{Weight of dish with insoluble ash} - \text{Weight of empty dish}}{\text{Sample weight}} \times 100.$$

$$\text{Water and alcohol soluble extractives} = \frac{\text{Weight of dish with sample after drying} - \text{Empty dish weight}}{\text{Sample weight} \times 25} \times 100$$

2.6. Phytochemical Screening

The phytochemical screening of the aqueous extract of *Hypericum perforatum* root was carried out by qualitative test to detect various phytoconstituents using the standard protocol (Anokwah et al., 2023; Faruq et al., 2024; María et al., 2018).

2.7. HPTLC Fingerprinting

2.7.1. Preparation of sample

Both root extracts of *Hypericum perforatum* (ethanol extract, sample No. 202507140105, and acetone extract, sample No. 202507140103) were weighed (100 mg) and dissolved in 10 mL of methanol to obtain suitable concentration for HPTLC analysis. Both sample solutions, ranging from 3 to 4 µL, were placed on HPTLC plate (Tiwari et al., 2025).

2.7.2. Preparation of reference solution

Standard solution of quercetin was prepared by dissolving 0.01 mg of pure quercetin in methanol. Different volumes (3–4 µL) of the standard were placed on HPTLC plates for calibration and comparison (Kumar et al., 2025).

2.7.3. Calibration and quantification

Samples and standards were applied using the CAMAG Linomat 5 applicator, which sprayed sample liquid into HPTLC plate in the form of narrow, uniform bands using an inert gas spray (typically nitrogen). The application was done at a dosage speed of 150 nL/s with a band length of 8 mm, ensuring precise and reproducible sample deposition. In stationary phase, silica gel 60 F254 HPTLC plates of 10 × 10 cm size were used. Mobile phase consisted of toluene–ethyl acetate–formic acid (ratio: 6:3.5:0.5). Development was carried out through glass chamber with 10 mL of the mobile phase, allowing the solvent front to move up to 80 mm on the plate. After development, the plate remained accomplished using an HPTLC scanner 3 at a wavelength of 254 nm under ultraviolet (UV) light for peak analysis and quantification (Hussain et al., 2022). Calibration parameters were set to single-level calibration using standard quercetin peaks. Peak height was used for quantification (Chen et al., 2021; Shah et al., 2022). Data filtering and baseline corrections were performed automatically with sensitivity settings optimized.

2.8. Liquid Chromatography–Mass Spectrometry (LC-MS) Analysis

Dried acetone and ethanol extracts were reconstituted in HPLC-grade methanol and filtered through 0.22-µm syringe filter. The sample was analyzed using LC-MS equipment with their electrospray ionization (ESI) sources, such as negative and positive ionization mode. Separation was attained on C18 reversed phase column maintained at 30°C with mobile phase of water and acetonitrile using gradient elution program. Flow rate was set at 0.3 mL/min and an injection volume of up to 10 µL. Mass spectrometer was operated in full scanning mode (50–1000 m/z) to detect a wide range of phytoconstituents (Yeniçeri et al., 2024). The resulting chromatogram and mass spectra were analyzed for peak identification using the National Institute of Standards and Technology (NIST) and literature databases.

2.9. Network pharmacology

2.9.1. Screening of bioactive compounds

The phytochemicals identified from *Hypericum perforatum* root extract using LC-MS analysis were selected for network pharmacology and gene ontology studies. The corresponding canonical simplified molecular input line entry system (SMILES), these phytochemicals were retrieved from PubChem database (https://pubchem.ncbi.nlm.nih.gov/) (John et al., 2024).

2.9.2. Finding potential targets and drug-related genes

Potential target genes were predicted by utilizing the Swiss target prediction (http://www.swisstargetprediction.ch/), a web tool that employed 2D or 3D molecular similarity algorithms to identify the most probable protein targets associated with bioactive small molecules. The output gene lists corresponding to phytochemicals were compiled for analysis. Disease-related genes associated with epilepsy were then retrieved from GeneCards database (https://www.genecards.org/), which provides comprehensive gene–disease associations based on integrative genomic and proteomic data. To identify common intersecting genes, lists obtained from Swiss target prediction and GeneCards were submitted to the Venny 2.1 web tool (https://bioinfogp.cnb.csic.es/tools/venny/), which modified visualization and extraction of common genes selected for construction of network (Mayr et al., 2020).

2.9.3. Network construction and gene ontology

Protein–protein interaction (PPI) networks and its phytochemicals–protein interaction analysis were performed using Cytoscape version 3.9.1 is a bioinformatic computational

platform for complex network visualization and analysis. The CytoHubba plugin was employed to rank and identify the top ten target proteins based on interaction scores using the 'Degree' algorithm which evaluates nodes according to their number of direct connections within the network connections (Ekkbal et al., 2024; Singh et al., 2024). Gene–disease interactions were identified using the DisGeNet database (Kumar et al., 2024) and the gene ontology-enrichment analysis was conducted through network analyst (https://www.networkanalyst.ca/) to elucidate biological processes, molecular functions as well as pathways significantly associated with the identified gene set (Aggarwal et al., 2025).

3. RESULTS

3.1. Morphological study

Hypericum perforatum root is brown in color, having rough surface, slender, irregular shape, and woody with many small, fibrous side roots and extensive creeping rhizomes. The root is approximate 4–5 cm in length (Figure 1 and Table 1).

3.2. Microscopical studies

3.2.1. Anatomical studies

The transverse section (TS) of mature *Hypericum perforatum* root revealed distinct secondary growth tissues. The secondary cortex forms the outer layer, followed inwardly by well-developed secondary phloem and secondary xylem, which facilitate nutrient and structural support, respectively. Prominent rays are observed extending radially through secondary tissues, aiding in lateral transport and storage (Figure 2).

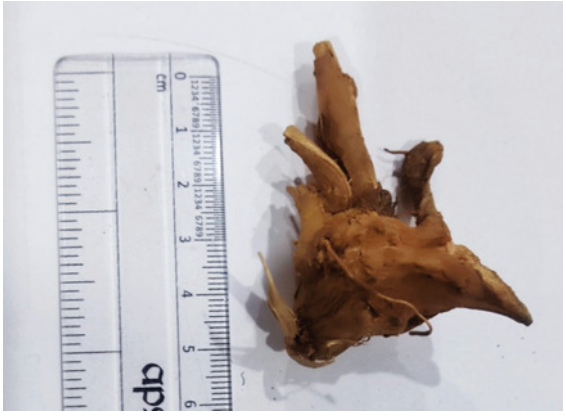

Figure 1. The dried root of *Hypericum perforatum*, shown alongside a metric ruler to indicate its size, shape, and external morphological characteristics.

Table 1
Organoleptic characteristics of *Hypericum perforatum* root.

Parameter	Observation
Color	Brown
Shape	Irregular
Size	Approximately 4–5 cm in length
Taste	First bitter, then slightly acrid or astringent
Odor	Pungent
Texture	Rough

3.2.2. Powder microscopy

Powder microscopy of *Hypericum perforatum* root revealed distinct anatomical features, such as (A) cortical parenchyma, (B) secondary cortex, and (C) secondary xylem fragments; (D) stone cells (D) were present indicating mechanical support, while (E) biseriate rays and (F) secondary phloem were also identifiable, reflecting the complex vascular structure of root tissue. These microscopic characteristics, as shown in Figure 3, help in the identification and standardization of the powdered drug material.

3.3. Phytochemical screening

Phytochemical screening of *Hypericum perforatum* extracts revealed that both ethanol and acetone extracts contained

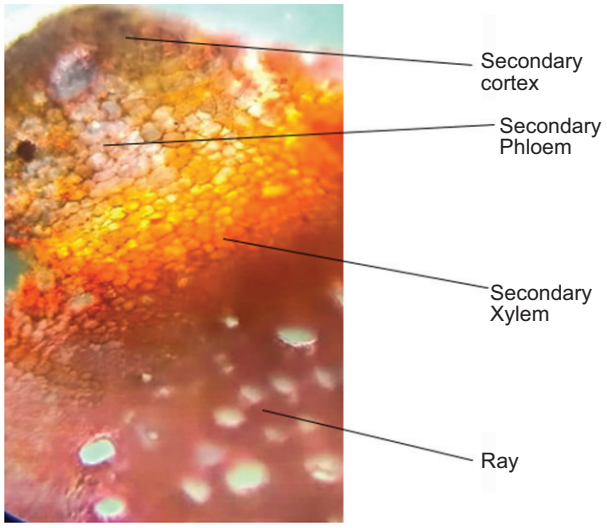

Figure 2. Transverse section (TS) of *Hypericum perforatum* root showing secondary cortex, secondary phloem, secondary xylem, and prominent medullary rays.

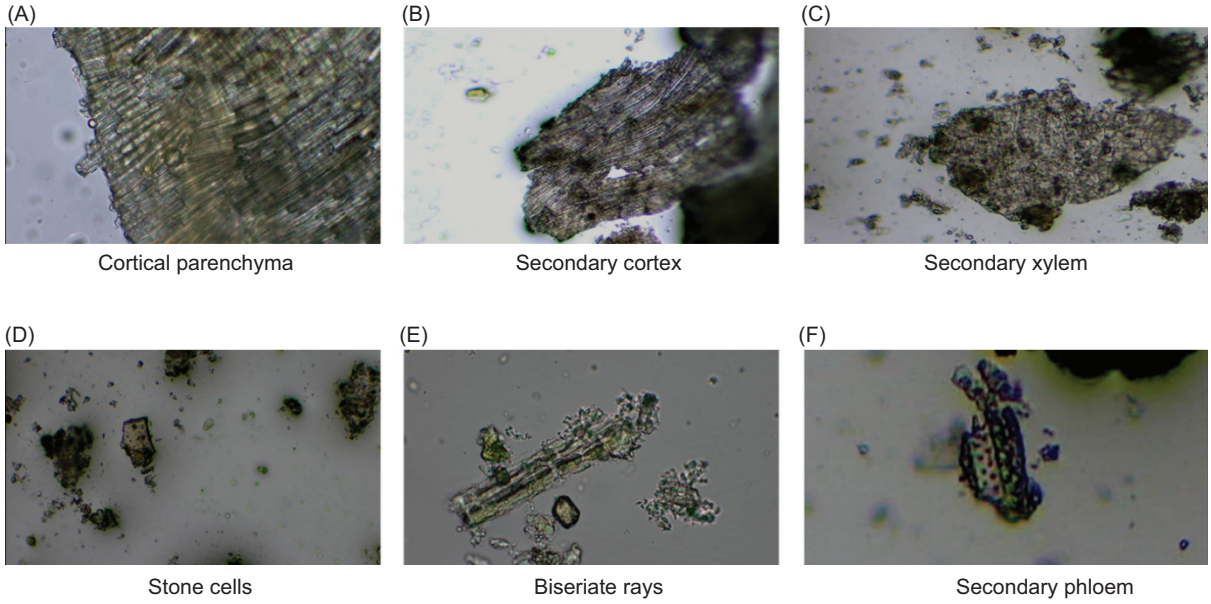

Figure 3. Powder microscopy of *Hypericum perforatum* shows (A) cortical parenchyma, (B) secondary cortex, and (C) secondary xylem; (D) stone cells are present, indicating mechanical support, with (E) biseriate rays and (F) secondary phloem.

alkaloids, amino acids and derivatives, phenols, and fatty acids. The ethanol extract was additionally positive for flavonoids, terpenoids, and anthocyanins, whereas acetone extract showed stronger presence of terpenoids and fatty acids, as cited in Table 2.

Table 2
Preliminary phytochemical screening of ethanol and acetone extracts of *Hypericum perforatum* indicating the presence (+), strong presence (++), or absence (-) of major classes of phytoconstituents.

S. No.	Phytochemical screening	Ethanol extract of *Hypericum perforatum*	Acetone extract of *Hypericum perforatum*
1.	Alkaloid	++	++
2.	Saponin	-	-
3.	Flavonoid	+	+
4.	Amino acid and derivatives	++	++
5.	Phenol	++	++
6.	Tannin	-	_
7.	Terpenoid	+	++
8.	Steroid	-	-
9.	Glycoside	-	-
10.	Anthocyanin	+	-
11.	Fatty acid	+	++
12.	Carbohydrate	-	-

3.4. Physiochemical Parameters

Physiocochemical analysis of *Hypericum perforatum* root showed a total ash content of 8.225 ± 0.212%, water-soluble ash as 3.252 ± 0.056%, and acid-insoluble ash as 1.106 ± 0,053%. The water-soluble extractive was 25.85 ± 0.884% and alcohol-soluble extractive was 20.764 ± 0.711%, while loss on drying was calculated as 9.832 ± 0.384%. All values were expressed as mean ± standard deviation, reflecting roots' compositional profile as determined by standard pharmacopeial methods shown in Table 3.

3.5. HPTLC fingerprinting analysis

High-performance thin-layer chromatography profiling were carried out on silica gel G60 F254 plates, with toluene–ethyl

Table 3
Physicochemical parameters of *Hypericum perforatum* root.

S. No.	Parameter	*Hypericum perforatum*
1.	Total ash value (%)	8.225 ± 0.212
2.	Water-soluble ash (%)	3.252 ± 0.056
3.	Acid-insoluble ash (%)	1.106 ± 0.053
4.	Water-soluble extractive (%)	25.85 ± 0.884
5.	Alcohol-soluble extractive (%)	20.764 ± 0.711
6.	Loss on drying (%)	9.832 ± 0.384

acetate–formic acid (ratio: 6:3.5:0.5) as mobile phase. Detection was performed at 254 nm. A quercetin standard (0.0100 mg) showed a characteristic band at a retention factor (Rf) value of 0.30. Both extracts of *Hypericum perforatum* root produced bands with Rf values closely matching that of quercetin as shown in Figure 4. The acetone extract (sample 202507140103) exhibited a prominent band at an Rf value of 0.29, with a peak height 32.9 and an area of 498.9 AU (arbitrary units), as shown in Figure 5. On the other hand, the ethanol extract (sample 202507140105) displayed a corresponding band at an Rf value 0.28, with a peak height of 21.7 and an area of 330.3 AU, as shown in Figures 4 and 5. Relative quantification against the single-level quercetin standard (area 10528.1 AU) indicated that the quercetin was present in both extracts. Comparison of peak areas of samples revealed that the acetone extract contained 1.5-fold higher levels of quercetin than the ethanol extract (498.9 ÷ 330.3 = 1.51) as shown in Table 4.

3.6. LC-MS analysis

Liquid chromatography–mass spectrometry analysis revealed the tentative identification of seven phytochemicals in extracts, including phenolic acids and flavonoids, based on the comparison of observed mass-to-charge ratio (m/z) values

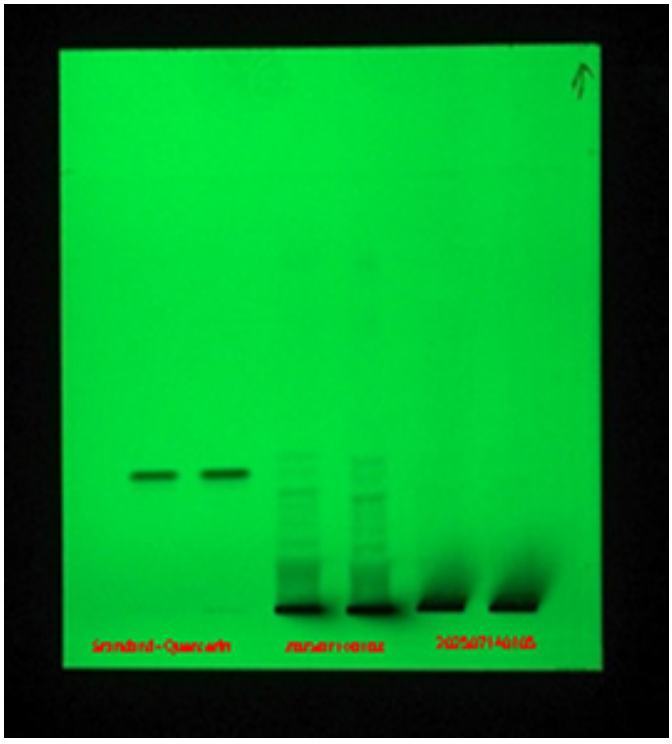

Figure 4. HPTLC fingerprint profiles of ethanol and acetone root extracts of *Hypericum perforatum* L. obtained under optimized chromatographic conditions.

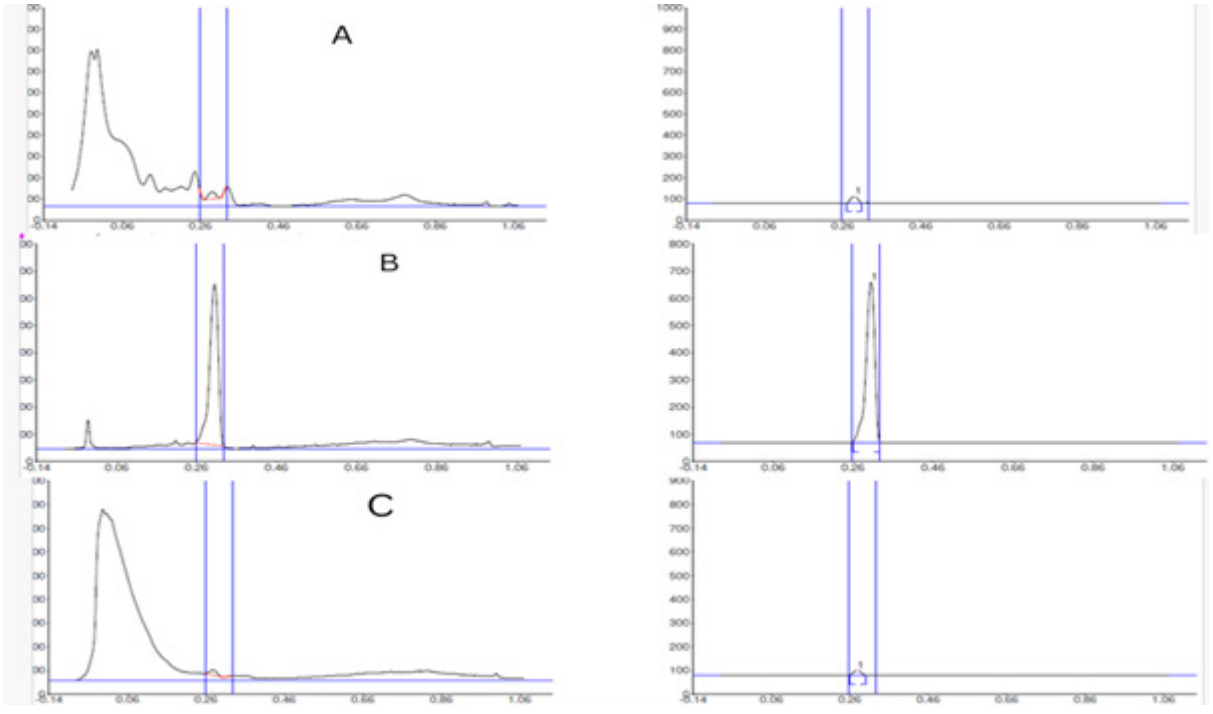

Figure 5. Densitometric HPTLC chromatograms of quercetin showing (A) standard quercetin and its corresponding peaks in (B) acetone extract and (C) ethanol extract of *Hypericum perforatum* roots. The standard quercetin exhibited a single well-resolved peak at an Rf value of 0.30, confirming its purity. Corresponding peaks observed at Rf = 0.29 in acetone extract and Rf = 0.28 in ethanol extract indicate the presence of quercetin with comparable chromatographic behavior.

Table 4
Densitometric HPTLC quantification parameters of quercetin in *Hypericum perforatum* root extracts.

Sample	Maximum Rf	Peak area (AU)	Area (%)	Interpretation
Standard quercetin	0.30	10528.1	100.00	Single sharp peak confirms purity and chromatographic specificity.
Acetone extract	0.29	498.9	100.00	Presence of quercetin corresponding to standard Rf.
Ethanol extract	0.28	330.3	100.00	Presence of quercetin with comparable chromatographic behavior.

Note: HPTLC: high-performance thin-layer chromatography; Rf: retention factor.

with theoretical masses and characteristic MS–MS fragmentation patterns. Gallic acid, caffeic acid, and ferulic acid were identified as deprotonated molecular ions $[M-H]^-$, showing diagnostic fragment ions arising from decarboxylation and neutral losses typical of hydroxybenzoic acid and hydroxycinnamic acid derivatives. Flavonoids, such as catechin/epicatechin, quercetin, and kaempferol, exhibited both protonated $[M+H]^+$ and deprotonated $[M-H]^-$ ions with fragmentation patterns consistent with Retro-Diels-Alder cleavages, yielding characteristic product ions at m/z 151 and 179. Rutin was identified by its molecular ions in both ionization modes and by sequential loss of sugar moieties producing the quercetin aglycone ion (m/z 303). An approximate 2-Da difference observed between ions in positive and negative modes corresponds to protonation and deprotonation processes during electrospray ionization. Overall, the close agreement between identified and theoretical masses, together with compound-specific fragmentation behavior, supports the reliable tentative identification of the phytochemicals listed in Table 5.

3.7. Network pharmacology

3.7.1. Screening of active compounds

A total of 1095 potential target genes were retrieved from the GeneCard database for further analysis. As shown in Figure 6, Venn diagram analysis identified 96 overlapping target genes by intersecting 1095 epilepsy-related targets, with 143 potential targets associated with the active compounds of *Hypericum perforatum.*

3.7.2. Constructions for protein–protein interaction

In a network analysis of PPI, 143 predicted targets were submitted to the STRING database, generating a network comprising 143 nodes and 1480 edges, with an average node of 20.7 integrating all available interactions of PPI enrichment and $p < 1.0 \times 10^{-16}$. Interaction data were subsequently imported into Cytoscape for visualization and topological analysis, where nodes represented targets, edges denoted interactions between targets, and edge thickness reflected interaction strength. To define the core PPI sub-network, CytoHubba was applied using the MCC algorithm, which identified the following top 10 nodes with highest centrality: *SRC*, *AKT1*, *ESR1*, *STAT3*, *BCL2*, *PTGS2*, Epidermal Growth Factor Receptor (*EGFR*), *TP53*, *MMP9*, and *ALB* (Figure 7). These key targets were then integrated into compound–target pathway for further study.

3.7.3. Integrated pathway enrichment analysis

Integrated pathway enrichment analysis of Kyoto Encyclopedia of Genes and Genomes (KEGG) pathway and gene ontology revealed that the identified targets participate in multiple biological processes relevant to epilepsy, including neuronal excitability, inflammation, oxidative stress, and cell survival. The KEGG pathway enrichment demonstrated significant involvement of endocrine resistance, estimated glomerular filtration rate (EGFR), and tyrosine kinase inhibitor resistance, oestrogen signaling, lipid atherosclerosis, and human cytomegalovirus infection pathways. These pathways are associated with neuroinflammatory signaling, hormone-mediated neuronal modulation, and dysregulated kinase activity, all of which contributed to epileptogenesis. In specifically, estrogen plays a important role in modulating synaptic plasticity and seizure susceptibility by regulating neuronal excitability and intracellular signaling mechanisms. Analysis of gene ontology highlighted response to oxidative stress, regulation of protein phosphorylation, and negative regulation of apoptotic and programmed cells death processes. These processes are involved in epilepsy, as oxidative stress and phosphorylation promote neuronal hyperexcitability and seizure-induced neuronal injury, while anti-apoptotic mechanisms may confer neuroprotection. Cellular component enrichment indicated localization of targets to membrane microdomains and nuclear membranes, suggesting involvement in receptor-mediated signaling and ion channel regulation. Molecular function analysis revealed enrichment in nitric oxide synthase regulator activity, kinase binding, and transcription factor binding. Overall, the integrated KEGG–GO analysis suggested that modulation of estrogen signaling,

Table 5
Liquid chromatography–mass spectrometry (LC-MS)-based profiling of phytochemicals identified in the extracts of *Hypericum perforatum* roots under positive and negative ESI mode.

Sr. No.	Phytochemical identified	PubChem compound identification (CID)	Chemical structure	Identified mass (m/z)	Theoretical mass (m/z)	Fragmentation (m/z)	Ionization mode
1.	Gallic acid	370	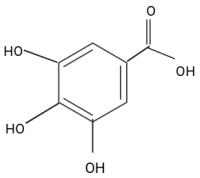	169.0	169.01 $[M-H]^-$	125.0, 97.0, 79.0	ESI -
				171.0	171.03 $[M+H]^+$	153.0, 125.0	ESI +
2.	Ferulic acid	445858	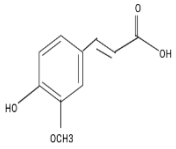	193.0	193.05 $[M-H]^-$	178.0, 160.0, 134.9	ESI -
				195.0	195.07 $[M+H]^+$	177.0, 149.0	ESI +
3.	Caffeic acid	689043	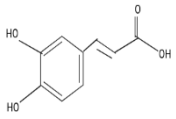	179.0	179.03 $[M-H]^-$	135.0, 107.0	ESI -
				181.0	181.05 $[M+H]^+$	163.0, 135.0	ESI +
4.	Catechin	9064	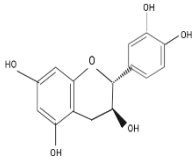	289.0	289.07 $[M-H]^-$	245.0, 205.0, 179.0	ESI -
				291.0	291.08 $[M+H]^+$	273.0, 245.0, 139.0	ESI +
5.	Quercetin	5280343	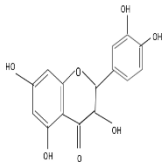	301.0	301.03 $[M-H]^-$	271.0, 179.0, 151.0	ESI -
				303.0	303.05 $[M+H]^+$	285.0, 257.0, 153.0	ESI +
6.	Kaempferol	5280863	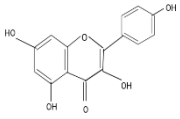	285.0	285.04 $[M-H]^-$	255.0, 227.0, 151.0	ESI -
				287.0	287.06 $[M+H]^+$	269.0, 241.0, 153.0	ESI +
7.	Rutin	5280343	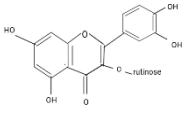	609.0	609.14 $[M-H]^-$	465.1, 303.0	ESI -
				611.0	611.16 $[M+H]^+$	465.1, 303.0	ESI +

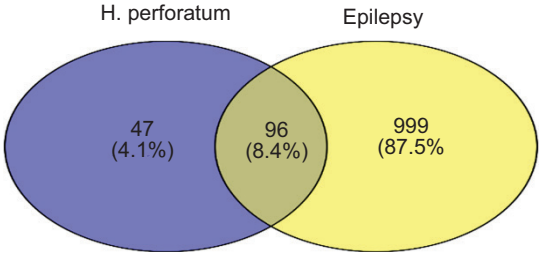

Figure 6. Venn diagram illustrating shared target genes between active compound-associated targets and disease-related genes representing potential therapeutic targets.

kinase-mediated pathways, oxidative stress responses, and apoptotic regulation represented key mechanisms underlying the potential of anti-epileptic effects of the identified phytochemicals as shown in Figure 8.

3.7.4. Compound-target interaction network analysis

Compound-target interaction network is constructed to elucidate its molecular interaction between its identified phytochemicals and epilepsy-related targets. The network demonstrates that gallic acid, ferulic acid, quercetin, kaempferol, and rutin interact with multiple protein targets, indicating

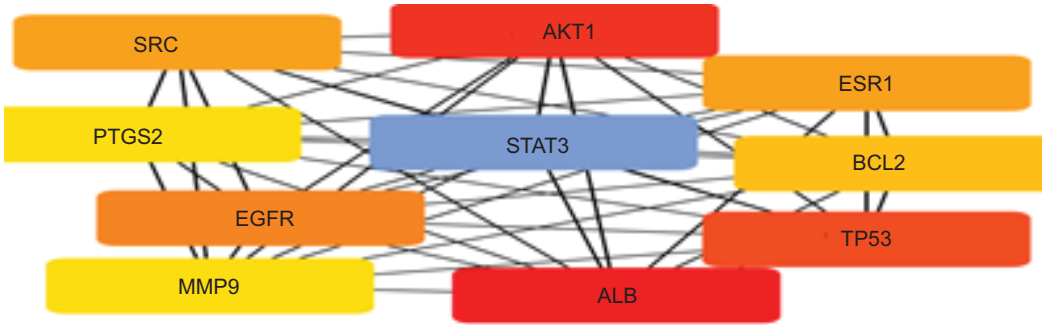

Figure 7. Core protein–protein interaction (PPI) network of 10 hub genes identified by using the CytoHubba plug-in Cytoscape software. The network pharmacology comprises *SRC*, *AKT1*, *ESR1*, *STAT3*, *BCL2*, *PTGS2*, *EGFR*, *TP53*, *MMP9*, and *ALB* as key hub nodes. Circular node represents individual proteins and edges, indicate that PPI illustrate the functional interconnectivity and central regulatory role of these targets within the network.

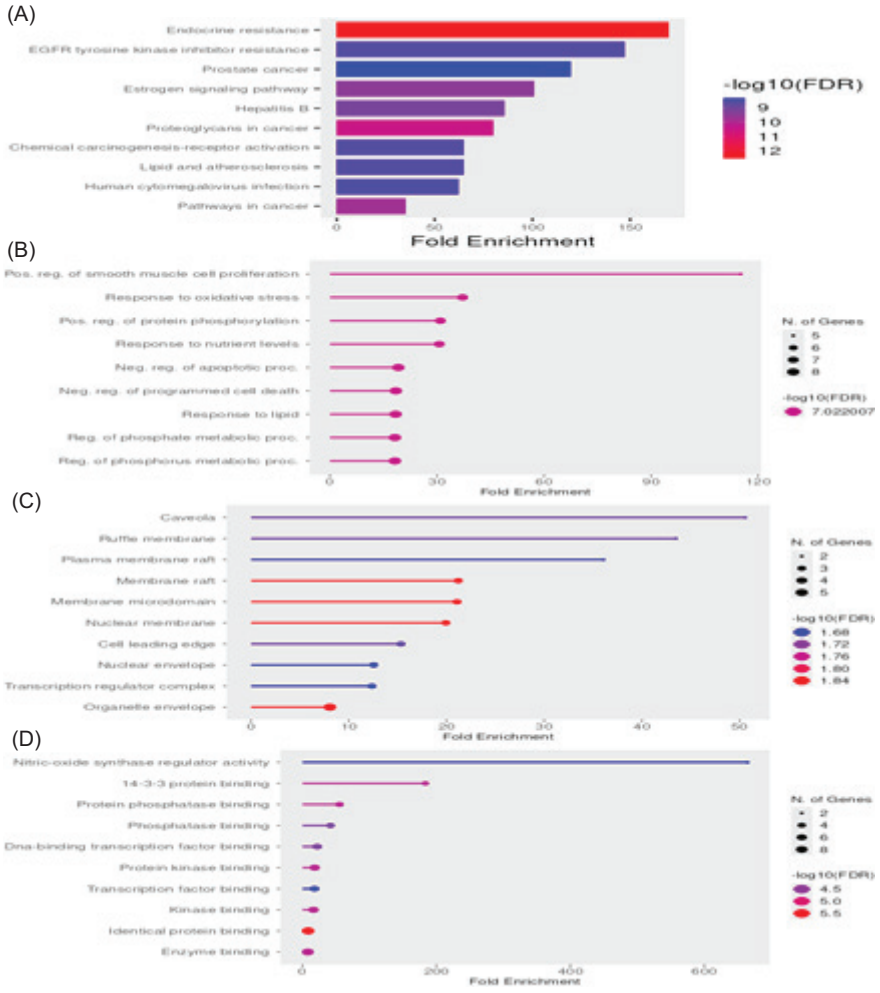

Figure 8. Integrated KEGG pathway and gene ontology analysis of core targets. (A) KEGG pathway enrichment shows significantly associated signaling pathways ranked by fold enrichment. (B) Gene ontology biological process enrichment highlights processes related to oxidative stress response, regulation of phosphorylation, and apoptosis. (C) Gene ontology cellular component enrichment indicates predominant localization of targets in membrane rafts, caveolae, and nuclear-associated components. (D) Gene ontology molecular function enrichment illustrates nitric oxide synthase regulator activity, kinase binding, and transcription factor binding.

a multi-target pharmacological profile. Among the targets, *SRC*, *AKT1*, *EGFR*, *STAT3*, *TP53*, *BCL2*, *PTGS2*, *MMP9*, *ESR1*, and *ALB* exhibited high connectivity, suggesting their central regulatory roles within the network. Quercetin and rutin showed strong interactions with several hub proteins, such as AKT1, EGFR, STAT3, and TP53, highlighting their potential importance in modulating key signalling pathways as shown in Figure 9. Presence of shared targets among multiple phytochemicals indicates possible synergistic effects. Furthermore, pathway associations, such as estrogen signaling and human cytomegalovirus infection pathways, suggest the involvement of these targets in inflammation, apoptosis, and neuroprotective mechanisms.

3.7.5. Gene–disease interaction

The disease–gene interaction network highlights *PTGS2* (COX-2) as a central hub gene linking multiple pathological conditions, indicating its pleiotropic role in disease modulation. *PTGS2* shows a strong association with status epilepticus, whereas its interaction with SRC suggested involvement of inflammatory and kinase-mediated signalling pathways, contributing to sustained neuronal excitation. In schizophrenia, *PTGS2* is connected with *ESR1*, suggesting a possible cross-link between neuroinflammation and estrogen-mediated neuroregulatory mechanisms. The network also links *PTGS2* to adenocarcinoma, where its interaction with anti-apoptic gene *BCL2* reflects a role in tumor progression through inflammation-driven cell survival and resistance to apoptosis. Overall, this interaction map demonstrates that *PTGS2* serves as a key molecular mediator bridging neurological disorders and cancer via shared inflammatory and signaling pathways, suggesting its significance as a potential therapeutic target, as shown in Figure 9.

4. DISCUSSION

Standardization of herbal drugs is essential for reproducibility, safety, and its therapeutic efficacy. In the present study, pharmacognostical and physicochemical parameters of *Hypericum perforatum* roots were systematically evaluated to establish baseline quality standards. Ash values and extractive values serve as fundamental indicators of purity, inorganic content, and solvent extractable constituents, which are used for detecting adulteration and ensuring raw material consistency. While LC-MS provides high resolution identification of phytoconstituents, HPTLC offers distinct advantages in herbal standardization, including visual fingerprinting, cost effectiveness, simplicity, and suitability for routine quality control. The densitometric HPTLC analysis confirmed the presence and purity of quercetin with consistent Rf values across ethanol and acetone extracts, thereby supporting marker-based standardization and batch-to-batch reproducibility. Such validation cannot be achieved by LC-MS alone, as LC-MS primarily focuses on compound identification rather than chromatographic consistency. LC-MS profiling revealed

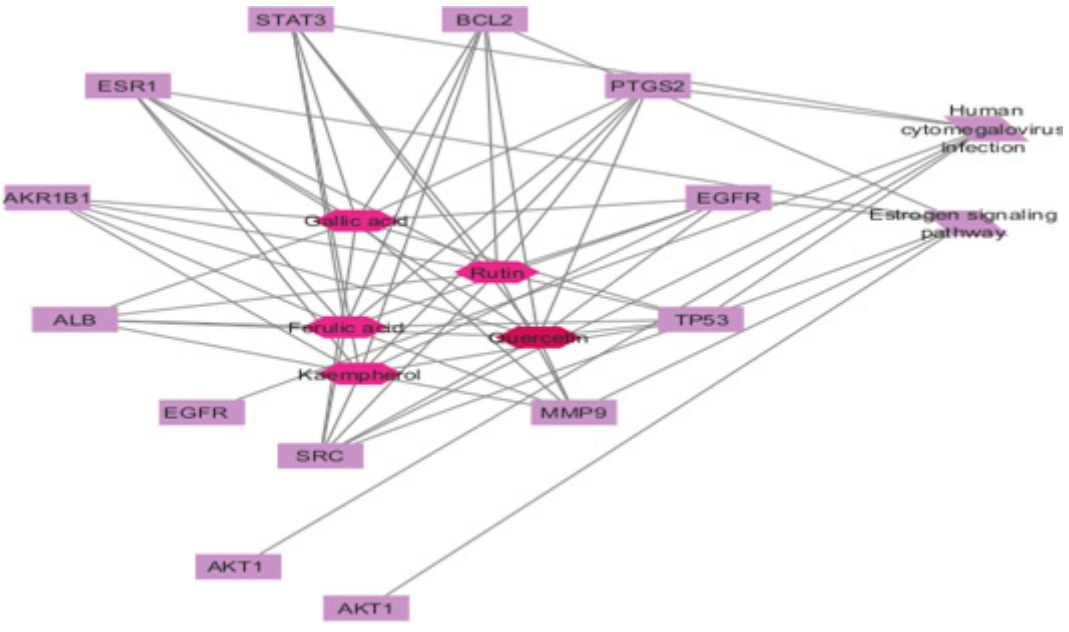

Figure 9. Compound-target interaction network illustrating relationships between identified phytochemicals and epilepsy-associated protein targets. Pink circular nodes represent phytochemical compounds, and purple rectangular nodes denote target proteins.

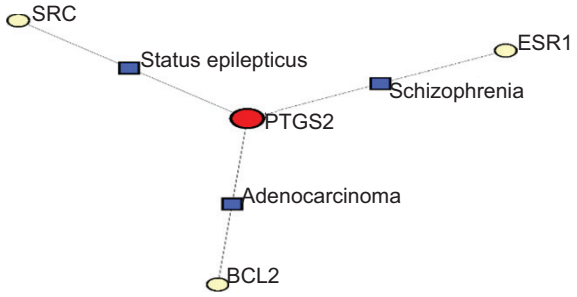

Figure 10. Disease–target interaction network showing *PTGS2* as a central hub linked to status epilepticus and related neurological conditions with interactions involving *SRC*, *ESR1*, and *BCL2*. Circular nodes represent target genes, square nodes denote disease phenotypes, and edges indicate reported associations.

the presence of flavonoids and phenolic acids known for neuroprotective, antioxidant, and anti-inflammatory activities.

Network pharmacology analysis further strengthened these findings by identifying hub targets, such as PTGS2, AKT1, EGFR, ESR1 and BCL2. These targets are documented in epileptogenesis, where neuroinflammation, oxidative stress, dysregulated kinase signaling, and impaired apoptotic balance play important roles. Integrated KEGG and gene ontology enrichment analysis demonstrated that estrogen signaling, EGFR tyrosine kinase pathways, oxidative stress response, and regulation of apoptosis are central mechanisms underlying the potential antiepileptic activity of *Hypericum perforatum*. The enrichment of targets within membrane rafts and caveolae indicates their involvement in ion channel regulation, a critical process underlying seizure initiation and propagation. Collectively, the results support a multi-target and multi-pathway mode of action consistent with phytotherapeutic principles.

5. CONCLUSION

The present investigation provides a comprehensive pharmacognostical, phytochemical, and mechanistic evaluation of *Hypericum perforatum* root extracts using an integrated bioinformatic strategy. Physicochemical parameters and preliminary phytochemical screening established essential quality control benchmarks, ensuring the authenticity and purity of plant material. The combined use of HPTLC and LC-MS proved important for standardization and phytochemical validation. HPTLC densitometric analysis played an important role in marker-based quality assessment by confirming the presence, purity, and chromatographic consistency of quercetin across different solvent extracts. Although LC-MS is a powerful tool for metabolite identification, it does not provide visual fingerprints or routine quality control metrics required for herbal drug standardization. Therefore, the inclusion of HPTLC besides LC-MS is scientifically justified and methodologically necessary, particularly for regulatory acceptance and reproducibility in herbal research. LC-MS analysis identified multiple bioactive phytochemicals with known neuroprotective potential. Network pharmacology and enrichment analysis revealed that these compounds collectively target key molecular pathways implicated in epilepsy, including neuroinflammation (PTGS2), oxidative stress response, kinase signaling (AKT1, EGFR, and SRC), estrogen-mediated neuronal modulation (ESR1), and apoptotic regulation (BCL2). These pathways are directly linked to neuronal excitability, synaptic plasticity, and seizure susceptibility. This study supports the therapeutic relevance of *Hypericum perforatum* roots as a multi-component, multi-target intervention for epilepsy.

ACKNOWLEDGMENT

The authors thanked IIMT College of Medical Sciences, IIMT University, Uttar Pradesh, India, for providing facilities and support to complete this study.

CONFLICT OF INTEREST

No conflict of interest declared.

ORCID

Pooja Sinoriya 0009-0002-3353-3551
Milind Sharad Pande 0000-0002-6065-4159
Nitin Kumar 0000-0003-4473-6418

AUTHOR CONTRIBUTIONS

Pooja Sinoriya: Research concept and design, collection and/or assembly of data, data analysis and interpretation, and critical revision of the article. Milind Sharad Pande: Final approval of the article. Nitin Kumar: Critical revision of the article.

REFERENCES

Abubakar A.R, H.M. 2020. Reparation of medicinal plants: Basic Extraction and Fractionation Procedures for Experimental Purposes.

Journal of Pharmaceutical and Biological Sciences. 12(1), 1–10. https://doi.org/10.4103/jpbs.JPBS_175_19

Adom, E., Ekuadzi, E., Boakye-gyasi, E., Kingsley, I. 2022. Phytomedicine plus pharmacognostic evaluation of three *Apocynaceae* plants that share the same West African local names. Phytomedicine Plus. 2(1), 100157. https://doi.org/10.1016/j.phyplu.2021.100157

Aggarwal, M., Ekbbal, R., Garg, G. 2025. Natural resources for human health *Angustifolia moench* for the treatment of myocardial infarction. February.

Alahmad, A., Al-zereini, W.A., Hijazin, T.J., Al-madanat, O.Y., Alghoraibi, I., Al-qaralleh, O., Al-qaraleh, S., Feldhoff, A., Walter, J., Scheper, T. 2022. Green synthesis of silver nanoparticles using *Hypericum perforatum* L. aqueous extract with the evaluation of its antibacterial activity against clinical and food pathogens. Pharmaceutics. 14(5), 1104. https://doi.org/https://doi.org/10.3390/ pharmaceutics14051104

Al Nooh, K.M., Salim, A.M., Faizy, W. S. et al. 2025. Synergistic effects of plant growth regulators and fe_3o_4 nanoparticles on *in vitro* organogenesis and bioactive compound production in hypericum perforatum. BMC Plant Biology. 25(1335), 1–14.

Amooaghaie, R., Rajaie, N. 2025. Foliar application of yeast extract mitigates water deficit stress and elicits hypericin and phenolic production in *Hypericum perforatum* L. Scientific Reports. 15, 20896. https://doi.org/https://doi.org/10.1038/s41598-025-06013-w

Anokwah, D., Asante-kwatia, E., Jibira, Y., Kingsley, I., Kyei, S., Pinkrah, G., Adzekey, B., Obese, E., Ofori, E., Peter, R., Yeboah, A. 2023. Pharmacognostic study and anti-inflammatory and antioxidant activities of *Loeseneriella africana*. South African Journal of Botany. 157, 174–188. https://doi.org/10.1016/j.sajb.2023.03.027

Behroozilak, M.A., Moftakharzadeh, S.A., Behroozlak, M., Vahedi, V., B.S. 2025. The influence of ethanolic extract of *Hypericum perforatum* (St. John's wort) on growth performance, serum metabolites, fat deposition, immunity, and lipid peroxidation in broiler chickens. Veterinary Medicine and Science. 11(5), e70507. https://doi.org/10.1002/vms3.70507

Borawska M.H., Naliwajko S.K., Moskwa, J., Markiewicz-Żukowska, R., Puścion-Jakubik, A.S.J. 2016. Anti-proliferative and anti-migration effects of Polish propolis combined with *Hypericum perforatum* L. on glioblastoma multiforme cell line U87MG. BMC Complementary and Alternative Medicine. 20(16), 367. https://doi.org/10.1186/s12906-016-1351-2

Chen, Y., Shan, C., Hoong, C., Fei, M., Wu, S. 2021. Development of a HPTLC method with iterative calibration approach for quantitative evaluation of kinsenoside content in different types of *Anoectochilus roxburghii*. Microchemical Journal. 165(February), 106076.

Coopoosamy, R., Singh, K., Naidoo, K., Nadasan, D.S. 2023. The role of phytomedicine: Bridging the gap between the past, present, and future. Journal of Medicinal Plants for Economic Development. 7(1), 1–7. https://doi.org/10.4102/jomped.v7i1.197

Dhanave, S.S., Mane, N.R., Shitole, P.D., Pore, A.V, Bais, S.K. 2024. Current Scenario Of Pharmaceutical And Herbal Medicines. International Journal of Pharmacy and Herbal Technology. 2(2), 1650–1656. ISSN No.: 2583-8962 (online).

Drożdżał, J., Barańska, O., Chańko, M., Krzaczkowski, A., Niedzielska, E., Rędaszka, M., Szuba, J., Szular, Z., Wojczulis, T., Ziemek, K. 2025. Hipercium species in the treatment of depression – A literature overview. Quality in Sport. 42, 60806. https://doi.org/10.12775/QS.2025.42.60806

Ekkbal, R., Gupta, P., Gyawali, R. 2024. System pharmacological approach to investigate and validate multitargeted and therapeutic effect of furocoumarins of *Apium graveolens* L. for treatment of kidney disease. Advances in Pharmacological and Pharmaceutical Sciences. 2024(1), 1–13. https://doi.org/10.1155/2024/5543561

Fan, S., Weng, W., Ji, S. 2024. Pharmacognostic studies on three species of *Spermacoce*. Journal of Holistic Integrative Pharmacy. 5(1), 2–9. https://doi.org/10.1016/j.jhip.2024.03.002

Faruq, M.O., Rahim, A., Arifuzzaman, M., Ghosh, G.P. 2024. Phytochemicals screening, nutritional assessment and antioxidant activities of A. viridis L. and A. spinosus L. leaves: A comparative study. Journal of Agriculture and Food Research. 18(May), 101341. https://doi.org/10.1016/j.jafr.2024.101341

Gempo, N., Yeshi, K., Jamtsho, T. 2024. Heliyon development of quality control parameters for two Bhutanese medicinal plants (Aster flaccidus Bunge and Aster diplostephioides (DC) Benth. ex C.B. Clarke) using traditional and modern pharmacognostical platforms. Heliyon. 10(3), e24969. https://doi.org/10.1016/j.heliyon.2024.e24969

Gokcek-Sarac C, Altunkaya G, K.S. 2025. Investigation of the anticarcinogenic effects of *Hypericum perforatum* extract on human thyroid cancer. Anti-Cancer Agents in Medicinal Chemistry. 25(10), 719–728. https://doi.org/10.2174/0118715206340411241120051020

Górnaś P, Mišina I, Perkons I, Segliņa D, C.-M. M. 2025. Characterization of tocochromanols in wild *Hypericum perforatum* populations in Latvia. Horticulturae. 11(2), 205. https://doi.org/https://doi.org/10.3390/horticulturae11020205

Górnaś P, Siger A. 2025. Rare prenyl lipids in wild St. John's wort during three harvest seasons. Molecules. 30(4), 901. https://doi.org/https://doi.org/10.3390/molecules30040901

Hussain, S., Azam, F., Mezogi, J., Abdmalla, F. 2022. A simple validated HPTLC method for the analysis of fl avonoids and molecular docking studies of novel tri-terpenoid glycoside isolated from *Carya illinoinensis* bark with potential anti-inflammatory and antinociceptive activities. South African Journal of Botany. 147, 596–607. https://doi.org/10.1016/j.sajb.2022.02.016

Jin, Z.J., Zhu, S.M., Luo, F.Y., Sun, Y., Gao, C.X., Feng, T., Ma, H., Xue, R., Li, C.W., An, L., Z. Y. 2025. A polysaccharide-rich ingredient from *Hypericum perforatum* L. ameliorates depression-like and post-traumatic stress disorder-like symptoms in mouse models. Nutrients. 17(20), 3222. https://doi.org/10.3390/nu17203222

John, I., Lagu, L., Nyamai, D.W., Njeru, S.N. 2024. Phytochemical analysis , *in vitro* and *in silico* study of antiproliferative activity of ethyl acetate fraction of *Launaea cornuta* (Hochst. ex Oliv. Hiern) C. Jeffrey against human cervical cancer cell line. Frontiers in Pharmacology. 81, 1–25. https://doi.org/10.3389/fphar.2024.1399885

Kilibarda, S., Jović, M.D., Milinčić, D.D., Vuković, S., Trifković, J.Đ., Pešić, M.B., K. A. 2025. Phytochemical profile and biological activities of Rtanj's *Hypericum perforatum* infusion tea and methanolic extracts: Insights from LC-MS/MS and HPTLC–Bioautography. Plants. 14(9), 1377.

Klangprapun, S., Buranrat, B., Caichompoo, W., Nualkaew, S. 2018. Pharmacognostical and physicochemical studies of *Enhalus acoroides* (L.F.) Royle (rhizome). Pharmacognosy Journal. 10(6), S89–S94. https://doi.org/10.5530/pj.2018.6s.17

Kumar, S., Narayana, K., Kaira, P., Karthikeyan, M. 2025. Integrating macro-microscopy, DNA barcoding and HPTLC for quality assessment of berberine containing botanicals traded as Maramanjal/

Daruharidra. Journal of Ayurveda and Integrative Medicine. 16(5), 101192. https://doi.org/10.1016/j.jaim.2025.101192

Kumar, A., Salar, S., Kumar, D., Aggarwal, M., Sharma, S., Ekbbal, R. 2024. Multi-targeted therapeutic exploration of *Tamarix gallica* flowers for anti-ulcer activity and associated complications. Journal of Ayurveda and Integrative Medicine. 15(4), 100947. https://doi.org/10.1016/j.jaim.2024.100947

Kurt, A.A., Ibrahim, B., Cinar, H., Ozmen, O. 2025. Enhanced therapeutic potential of *Hypericum perforatum* L.: A comprehensive *in vitro* and *in vivo* evaluation of nanoparticle-hydrogel formulations. Journal of Nanotechnology. 6232038(1), 1–16. https://doi.org/10.1155/jnt/6232038

Limpabandhu, T., Suwatronnakorn, M., Prasansuklab, A. 2024a. Phytomedicine plus pharmacognostic standardization and phytochemical evaluation of *Ficus rumphii* blume leaves in Thailand. Phytomedicine Plus. 4(4), 100661. https://doi.org/10.1016/j.phyplu.2024.100661

Limpabandhu, T., Suwatronnakorn, M., Widoyanti, A.A.E., Issaravanich, S., Zongrum, O., Prasansuklab, A. 2024b. Pharmacognostic standardization and phytochemical evaluation of *Ficus rumphii* blume leaves in Thailand. Phytomedicine Plus. 4(4), 100661. https://doi.org/10.1016/j.phyplu.2024.100661

Ma, X., Chen, N., Zeng, P., He, Y., Zhang, T., Lu, Y., Li, Z., Xu, J., You, J., Zheng, Y., Wang, L., Luo, M., W. J. 2025. *Hypericum perforatum*-derived exosomes-like nanovesicles: A novel natural photosensitizer for effective tumor photodynamic therapy. International Journal of Nanomedicine. 4(20), 1529–1541. https://doi.org/10.2147/IJN.S510339

María, R., Shirley, M., Xavier, C., Jaime, S., David, V., Rosa, S., Jodie, D. 2018. Preliminary phytochemical screening, total phenolic content and antibacterial activity of thirteen native species from Guayas province Ecuador. Journal of King Saud University – Science. 30(4), 500–505. https://doi.org/10.1016/j.jksus.2017.03.009

Maslov O, Komisarenko M, Ponomarenko S, Haltseva O, O.T. 2025. Investigation of the correlation between the antioxidant, antimicrobial activity and the content of phenolic compounds of St. John`s wort (*Hypericum perforatum* L.) liquid extracts. Pharmakeftiki. 37(3), 237–247.

Mayr, F., Möller, G., Garscha, U., Fischer, J., Rodr, P., Inderbinen, S.G., Temml, V., Waltenberger, B., Schwaiger, S., Hartmann, R.W., Gege, C., Martens, S. 2020. Finding new molecular targets of familiar natural products using *in silico* target prediction. International Journal of Molecular Sciences.

Monagas, M., Brendler, T., Brinckmann, J., Dentali, S., Gafner, S., Giancaspro, G., Johnson, H., Kababick, J., Ma, C., Oketch-rabah, H., Pais, P., Sarma, N. 2022. Understanding plant to extract ratios in botanical extracts. Fronteirs in Pharmacology. 70(September), 1–10. https://doi.org/10.3389/fphar.2022.981978

Palaiogiannis, D., Chatzimitakos, T., Athanasiadis, V., Bozinou, E., Makris, D.P., Lalas, S.I. 2023. Successive solvent extraction of polyphenols and flavonoids from *Cistus creticus* L. leaves. Oxygen. 3(3), 274–286. https://doi.org/10.3390/oxygen3030018

Rayhaneh Amooaghaie, N.R. 2025. Exploring effect of chitosan on antioxidant system and hypericin content in *Hypericum perforatum* L. under various irrigation regimes. BMC Plant Biology. 25(1), 1–16. https://doi.org/10.1186/s12870-025-06887-y

Rizzo, P., Altschmied, L., Ravindran, B.M., Rutten, T., D. J. 2020. The biochemical and genetic basis for the biosynthesis of bioactive compounds in *Hypericum perforatum* L., one of the largest medicinal crops in Europe. Genes. 11(10), 1210. https://doi.org/10.3390/genes11101210

Schmidt-Przewoźna, K., Alam, M.M., Kicińska-Jakubowska, A., Romanowska, B. 2025. Eco-friendly dyeing plants with medicinal properties St. John's wort (*Hypericum perforatum* L.) and juniper (*Juniperus communis* L.) as a good material for textile applications. Journal of Natural Fibers. 22(1), 265659.

Shafaei, M. 2026. Effect of different drying methods on hypericin quantity in adventitious roots of St. John's wort (*Hypericum perforatum* L.) Wort. 8(2).

Shah, H., Naseer, A., Gupta, N., Singh, R. 2022. A study on HPTLC quantification for quality control of Myricetin, a nutraceutical from different plant parts of *Myrica esculenta Linn*. Biomedical and Pharmacology Journal. 15(March), 219–228.

Singh, R., Sahu, N., Tyagi, R., Alam, P., Akhtar, A., Walia, R., Chandra, A., Madan, S. 2024. Integrative network pharmacology, molecular docking, and dynamics simulations reveal the mechanisms of *Cinnamomum tamala* in diabetic nephropathy treatment: An *in silico* study. Current Issues in Molecular Biology. 46(11), 11868–11889. https://doi.org/10.3390/cimb46110705

Suryawanshi, M.V., Gujarathi, P.P., Mulla, T., B. I. 2024. *Hypericum perforatum*: A comprehensive review on pharmacognosy, preclinical studies, putative molecular mechanism, and clinical studies in neurodegenerative diseases. Naunyn-Schmiedeberg's Archives of Pharmacology. 397(6), 3803–3818. https://doi.org/10.1007/s00210-023-02915-6

Swingle, C., Ronald, A., Angie, T., Tusiimire, J., Sharon, V., Olusoji, C., Ronald, J., Alamin, A., Godwin, A., Engeu, P. 2024. Phytomedicine plus pharmacognostical evaluation and description of the leaf and root bark of. Phytomedicine Plus. 4(4), 100636. https://doi.org/10.1016/j.phyplu.2024.100636

Theodorakopoulou, A., Pylarinou, I., Anastasiou, I.A. 2025. The putative antidiabetic effect of *Hypericum perforatum* on diabetes mellitus. Cvd, 1–19.

Tiwari, R., Parvez, M.K., Babu, M.A., Al-Dosari, M.S., Singh, T.G., Goel, K.K., Ali, N., Tyagi, Y., Yadav, U., Kumar, B., Bansal, N. 2025. HPTLC- and LCMS-based investigation of ethanolic leaf extracts of *Nerium oleander* and identification of quercetin as potent compound targeting plasmodium proteases: An analytical and *in silico* approach. South African Journal of Botany. 183, 42–50. https://doi.org/10.1016/J.SAJB.2025.05.024

Yeniçeri, E., Altay, A., Koksal, E., Altın, S., Taslimi, P. 2024. Phytochemical profile by LC-MS/MS analysis and evaluation of antioxidant, antidiabetic, anti-Alzheimer, and anticancer activity of *Onobrychis argyrea* leaf extracts. European Journal of Integrative Medicine. 66(January), 102337.